PUBLICATIONS OF THE
ASTRONOMICAL SOCIETY OF THE PACIFIC

Vol. 72 August 1960 No. 427

RADIO SOURCE MEASUREMENTS AT 960 MC/S

D. E. HARRIS AND J. A. ROBERTS
California Institute of Technology Radio Observatory
Owens Valley, California

I. INTRODUCTION

The major surveys of radio sources made at meter wavelengths have shown a disquieting lack of agreement,[1] and an independent study of these sources using as simple an antenna as possible seems to be desirable. As a partial step in this direction, we report here a study of 106 radio sources made with one of the equatorially mounted 90-foot paraboloids of the Owens Valley Radio Observatory. This investigation was made at a frequency of 960 Mc/s.

The primary result of the study is a reliable catalogue of sources that will be used as a "finding list" for precise position measurements currently being undertaken with the two antennas operating as an interferometer. In addition, however, the results provide valuable information on the spectra of the sources, and have also been used in a search for optical counterparts to the sources.

Ninety of the objects observed were taken from the Third Cambridge Survey (3C),[2] which was kindly made available to us prior to its publication. The remaining 16 objects in the present list were either taken from other catalogues or were discovered in the course of the present investigation.

The equipment is briefly described in Section II, and in Sections III and IV the methods of determining the positions and intensities of the sources are outlined. In Section V suggested optical identifications are discussed, while Section VI is devoted to a consideration of the spectra of the sources. The positions, intensities, spectral indices, and other pertinent data for the 106 sources are collected in Table I, which will be found at the end of the article (p. 248).

II. EQUIPMENT

The 90-foot parabolic reflector was fed by a waveguide horn giving a tapered illumination that fell to approximately 10% at the edges of the reflector. The resulting main beam was nearly circular and 0°8 wide between half-power points, while the first sidelobe was approximately 1% of the main beam.

The receiver was of the comparison type, switching at 400 cps between the horn and a reference load. Initially this reference was a second horn mounted near the focus but directed away from the reflector. Later a resistor immersed in liquid nitrogen was used. This latter arrangement was less sensitive to external interference and less affected by variation in ground radiation as the antenna was moved.

The rf switch was of the quarter-wave variety and used gold-bonded germanium diodes as the switching elements. Special impedance-transforming sections were included between both the switch and the crystal mixer, and the mixer and the first i.f. amplifier, to insure optimum signal-to-noise conditions. The switch, mixer, and i.f. amplifier were mounted together in a box immediately behind the horn. The rest of the receiver was located inside the base tower of the antenna.

No image rejection was employed, so that both sidebands were utilized. The intermediate frequency was initially 30 Mc/s, but was later reduced to 10 Mc/s. In each case the bandpass was approximately 8 Mc/s wide, and the output time constant used was from 1 to 20 sec. The noise temperature of the receiver, as measured with a discharge tube noise generator, was approximately 300° K when the intermediate frequency was 30 Mc/s, and 200° K when the intermediate frequency was 10 Mc/s. The combination of the rf switch and interconnecting cables added approximately 90° K to the system temperature.

III. POSITION MEASUREMENTS

The apparent right ascension of a source was measured from a drift curve made with the antenna stationary and set on the 3C declination. From this record we determined the right ascension of a point midway between positions on either side of the source maximum and having equal amplitudes above a straight baseline of best fit (Figure 1*c*). Several such determinations were made

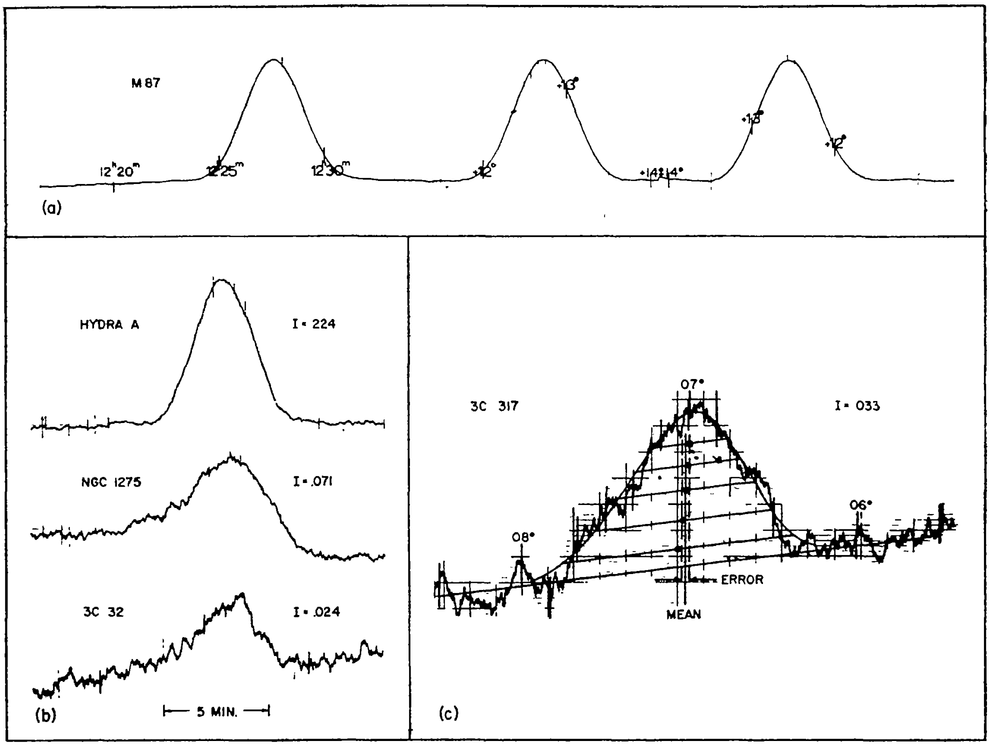

FIG. 1.—(*a*), Form of records used for position measurements. A drift curve is followed by two records made with the antenna tracking the source while being driven north and south at a rate of 1° in four minutes. (*b*), Examples of records used for intensity measurements showing the signal to noise ratio. The source intensity relative to M 87 is shown in the figure. The time constant was 20^s in all cases. (*c*), Method of analyzing the records for source position.

using points of different amplitude, and the mean of these was taken as the right ascension of the source. A reading error was assessed from the scatter of the individual determinations and was chosen so as to include approximately three-quarters of the points.

The declination was derived in a similar way from records made with the antenna tracking the correct right ascension while being driven in declination (both north and south) at a rate of 1° in four minutes.

The observed positions were corrected for refraction, precession, and errors in the telescope dials. These dial errors were determined each night by observing at least four of the five standard sources: the Crab Nebula, the Orion Nebula, M 87, Cygnus A and Cassiopeia A. These were chosen as position calibrators because of their strength, known optical position, and distribution over the sky. The dial errors for both right ascension and declination were found to be slow functions of declination; the right-ascension error varied by a total of $\sim 15^s$ and the declination error by $\sim 5'$ over the 65° range of declination covered by the calibrators.

The error assigned to a position observation was assessed as the sum of the reading error referred to above and an error due to the uncertainty of interpolation in the dial correction curves. Sources south of $\delta = -10^\circ$ suffer from an additional uncertainty due to the lack of calibrators, and the estimates of error for these sources have been increased accordingly. Usually two or three observations were obtained for each source, and the quoted error is estimated from the individual errors and the extent of agreement among the observations. It is felt that the probability of finding a source within the quoted error limit is about 80%.

IV. INTENSITY MEASUREMENTS

Intensities were measured by setting the antenna at the declination of the source and about 12^m ahead in right ascension and noting the deflection of the output recorder as the source drifted through the antenna beam. For most of the sources the declination used was determined from the observations described in Section III. However, for a number of the weaker sources, position measurements were not made and the Cambridge declination was used. Figure 1*b* shows examples of the drift curves from which the intensity measurements were made.

All source intensities were measured relative to M 87 (Virgo A), which is one of the standard sources recommended by the I.A.U. and which was available during the night for the larger part of the program. During that part of the year when M 87 was not available at night, secondary calibrators, Cygnus A and the Crab Nebula, were used. Absolute measurements were not attempted and where flux densities are quoted in this paper they are based on an assumed value for M 87 of 300×10^{-26} watts $m^{-2}(c/s)^{-1}$. This value was derived from published spectral data.[3,4] Other estimates of the flux from M 87 were made from the measured ratio to Cassiopeia A and its published spectrum, from the measured ratio to the moon, assumed to be at a temperature of 250° K, and from an estimate of the receiver noise and antenna efficiency. These methods all gave figures consistent with the above value. Flux densities are included in Table I on the basis of this figure, but it should be borne in mind that the intensity relative to M 87 is our observed quantity.

The intensity ratios given in Table I are average values from several observations and the quoted errors are estimated such that about three-quarters of the individual values lie within the limits of error. Thus, these errors are a measure of internal consistency and do not encompass systematic errors. One possible cause of systematic error is the use of a wrong declination for sources whose position we did not measure.

For all but the strongest sources the deflection of the output meter was proportional to the input power. However, for Cassiopeia A, Cygnus A, and the Crab Nebula the antenna temperatures were comparable with the receiver temperature so that departures of the detector characteristic from a square law became important. Correction factors for these sources were determined by measuring the detector law with a variable-precision attenuator inserted between the two i.f. amplifiers. As a check on this method, a further series of observations of these sources was made with a fixed attenuator inserted between the horn and the rf switch, and with the nitrogen load replaced by a reference at ambient temperature. This arrangement increased the receiver temperature and reduced the effective antenna temperatures of these sources to such an extent that the detector law was unimportant.

The final intensity ratios for the strongest sources are weighted means of all the observations and are believed to be accurate to 5%.

V. OPTICAL FIELDS

The plates of the National Geographic Society–Palomar Observatory Sky Survey were examined in a search for optical counterparts to the sources listed in Table I. For this purpose use was made of all available data on the radio sources, including preliminary measurements with the two 90-foot antennas operating as an interferometer. Details of this work, which is still continuing, will be published later. We have included in Table I an indication of the nature of the optical field in the neighborhood of the source, and in the cases of possible identification some details are given in the notes to Table I.

The nature of the optical field near each source is indicated in Table I by the Roman numerals I to IV in the final column. These symbols have the following significance:

I. A prominent or isolated extragalactic object near the radio position (possible identification).

IIa. Several bright objects within the limits of error: a more accurate position ($\pm 0\overset{\prime}{.}5$) could lead to an identification.

IIb. Several bright objects so close together that positional accuracy better than $\pm 0\overset{\prime}{.}5$ would be required to make an identification.

III. Only faint objects near the position.

IV. Heavy absorption in the region; no galaxies visible.

Many of the class I objects have been discussed previously by Minkowski[5,6] or by Dewhirst.[1,2,7]

VI. SPECTRA

By comparing the source intensities measured in the present investigation with those reported in the Cambridge surveys at 159 or 178 Mc/s,[2,7]* we obtained special information for the 90

* We wish to thank Drs. Elsmore, Ryle, and Leslie for communicating their results to us in advance of publication.

sources common to the two programs. The data were fitted to an assumed spectrum of the form

$$\text{flux density} \propto (\text{frequency})^x,$$

where x is termed the spectral index. As the present intensities were measured relative to M 87, the spectral indices quoted in Table I are those relative to M 87, i.e., they are $x - x_{M\,87}$. The spectral index of M 87 itself has been given as -0.74 by Whitfield,[3] and the 3C and Elsmore *et al.* values for the flux of M 87, taken in conjunction with our adopted 960 Mc/s value, yield indices of -0.72 and -0.70, respectively.

The distribution of the 90 values of the relative spectral index is shown in Figure 2*a*. There is seen to be a close clustering about the median value of $+0.1$ (a spectrum slightly flatter than that of M 87). About 10% of the values form a tail on the positive side, corresponding to spectra that are flatter than that of M 87, or increase with frequency.

At the other extreme, the steepest spectrum measured had an index relative to M 87 of -0.5, or an absolute spectral index of ~ -1.2. This is contrary to the conclusions of Whitfield, who found that 25% of the sources he studied had spectral indices steeper than -1.2 and that a few were as extreme as -1.8.[3] All but one of these sources are included in the present study. Provided only that the source spectra follow approximately a power law, it seems that the present indices, based on intensities at two widely spaced frequencies, will be subject to considerably less error than those derived by Whitfield, which often were based on intensities at a few closely spaced frequencies. For this reason we believe that the distribution of spectral indices shown in Figure 2*a* approaches the true distribution more closely than the distribution given by Whitfield.

The question then arises: How nearly does the present histogram approximate the true distribution and to what extent is it broadened by errors in the observations? In Figure 2*a*, 75% of the spectral indices lie within ± 0.25 of the median value. From the errors assigned to the two sets of observations one would expect a spread in which 75% of the spectral indices lay within ± 0.15 of their true value. This is sufficiently less than the ob-

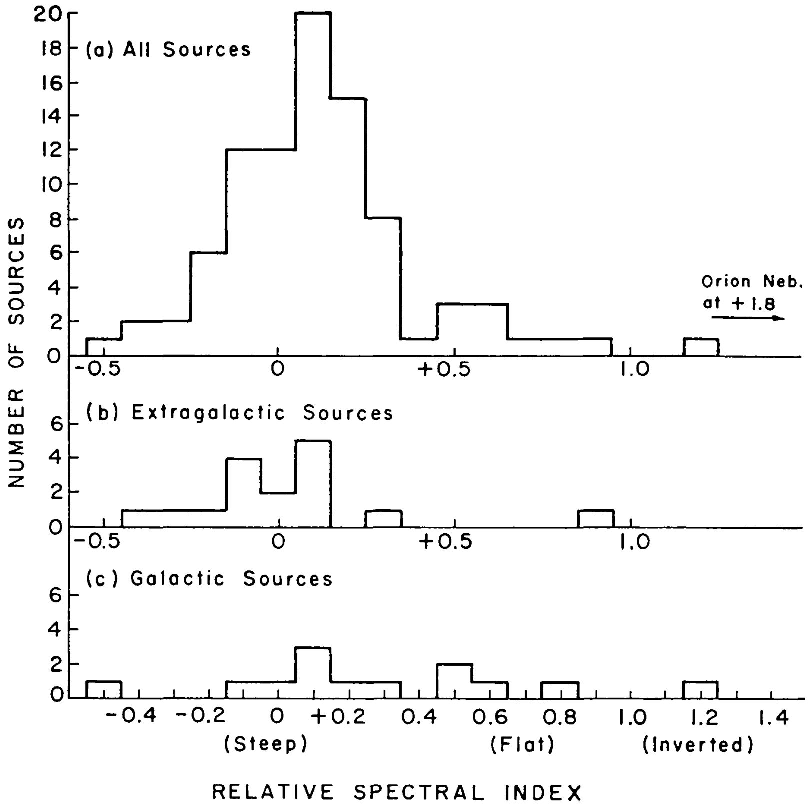

FIG. 2.—Histograms of relative spectral index ($x - x_{M87}$). (a), The 90 sources common to this paper and the recent Cambridge lists.[2,7] (b), The 5 well-known extragalactic sources, together with 11 probable identifications of galaxies (the Class I objects in Table I). (c), Galactic objects for comparison with (b). These sources include all objects in (a) that have $b \leqslant 10°$ and a diameter (Cambridge value) of 3′ or more, together with Kepler's supernova.

served spread to suggest that the errors do not broaden the observed distribution very markedly. This point was further tested by subdividing the data according to the magnitude of the errors in the flux measurements. For each of these subgroups the spread of the distribution obtained was substantially the same, again implying that the errors do not make a major contribution to the width of the observed distribution.

In a search for systematic differences in spectral index between different classes of objects, similar histograms were constructed with the sources grouped according to (1) intensity, (2) diameter (Cambridge data), and (3) galactic latitude. Although the grouping according to intensity suggests that the weaker sources may have slightly steeper spectra, the only grouping that yields a significant difference is the division into galactic and extragalactic objects. This separation is shown in the histograms of Figures *2b* and *2c*. Although the number of sources is too small for quantitative conclusions, the figures certainly suggest that the spectral indices of galactic objects are scattered over a much wider range than those of extragalactic objects. Thus all of the extragalactic spectral indices, except for 3C 270, lie within ± 0.35 of the index for M 87, and if the intensity given by Mills *et al.*[8] is used for 3C 270, its index also falls within this range.*

Those sources in Figure *2a* having extreme spectral indices were studied in more detail. Of the eleven sources with relative spectral indices $> +0.45$ ("flatter" spectra), four are identified galactic sources whose spectrum is well established (the Orion Nebula, the Rosette Nebula, the Crab Nebula, and IC 443). For the other seven sources alternative indices were computed by using the present 960 Mc/s intensities in conjunction with either the 81.5 Mc/s intensities of the 2C survey,[9] the 85 Mc/s intensities of Mills *et al.*,[8] or the 169 Mc/s intensities of Boischot.[10] In most cases, these alternative values were $< +0.45$, suggesting that the measurements are confused in some way. However for 3C 58 and 3C 398 even the alternative values are $> +0.6$. As both of these sources lie close to the galactic plane and have diameters of several minutes of arc, they are very probably galactic objects.

Of the five sources with excessively steep spectra (relative index < -0.25), only for 3C 28 do the alternative values confirm the index (-0.4). However, in this case the 960 Mc/s intensity may be too low as the position of this source was not measured in the present program.

VII. CONCLUSIONS

This study has demonstrated the general reliability of the Third Cambridge Catalogue, and indirectly confirmed the (relative) intensities of that catalogue by the narrow range of spectral

* Preliminary Caltech diameter measurements suggest that the 3C intensity may be low because of partial resolution of the source.

indices deduced in Section VI. Only one 3C source (3C 442) was not found, although for 3C 382 and 3C 384 a single source was found at an intermediate position (an alternative suggested in the 3C catalogue). 3C 442 was later found one lobe north of the quoted 3C position. A detailed comparison of the positions reveals that of the 69 sources from the 3C catalogue whose positions were measured in the present program, only 46 (67%) agree within the sum of the errors. Most of the disagreements are in right ascension only. For about half of these cases of disagreement, the positions have also been measured by either Elsmore *et al.*[7] or Mills *et al.*[8] Their measurements did not consistently agree with either the 3C values or the present observations. The present study, in conjunction with the Cambridge survey, has also shown that the spectral indices of the majority of the sources lie within a surprisingly small range. The median index is approximately −0.6, and 80% of the values lie between −0.3 and −0.9 (Section VI). This result has an important bearing on theories of the generation of nonthermal radio emission. Under fairly general conditions for the synchrotron theory, it implies that the distribution of electron energies must be similar in all of the sources.

The classification of the optical fields given in Table I provides a useful indication of the sources for which more accurate position measurements are most likely to prove fruitful (classes I and II). Our examination of the 48-inch Schmidt plates supports the idea that extragalactic radio sources tend to be associated with elliptical galaxies, and particularly with double and multiple systems.[1]

This investigation formed part of the program of the Owens Valley Radio Observatory and was carried out under U.S. Office of Naval Research contract Nonr-220(19). We are grateful to Professor J. G. Bolton for his guidance and encouragement in this work; to Mr. G. J. Stanley, who was responsible for the receiving equipment; to Mr. B. G. Clark for his help in examining the Schmidt plates; and to our several colleagues for their assistance in the observational program.

[1] See, e.g., D. W. Dewhirst, in *Paris Symposium on Radio Astronomy,* R. N. Bracewell, ed. (Stanford, Calif.: Stanford University Press, 1959), p. 507.

[2] D. O. Edge, J. R. Shakeshaft, W. B. McAdam, J. E. Baldwin, and S. Archer, *Mem. R.A.S.,* **68,** 37, 1959.

[3] G. R. Whitfield, *M.N.R.A.S.,* **117,** 680, 1957.

[4] C. H. Seeger, U.R.S.I. Commission V, Report from Subcommission V*d,* June 1957.

[5] R. Minkowski, *Pub. A.S.P.,* **70,** 143, 1958.

[6] R. Minkowski, *Proc. Nat. Acad. Sci.,* **46,** 13, 1960.

[7] B. Elsmore, M. Ryle, and P.R.R. Leslie, *Mem. R.A.S.,* **68,** 61, 1959.

[8] B. Y. Mills, O. B. Slee, and E. R. Hill, *Aust. J. Phys.,* **11,** 360, 1958.

[9] J. R. Shakeshaft, M. Ryle, J. E. Baldwin, B. Elsmore, and J. H. Thomson, *Mem. R.A.S.,* **67,** 106, 1955.

[10] A. Boischot, in *Paris Symposium on Radio Astronomy,* R. N. Bracewell, ed. (Stanford, Calif.: Stanford University Press, 1959), p. 492.

[11] G. Westerhout, *B.A.N.,* **14,** 215, 1958 (No. 488).

[12] R. Hanbury Brown and C. Hazard, *M.N.R.A.S.,* **113,** 123, 1953.

[13] V. F. Gaze and G. A. Shaïn, *Pub. Crimean Astrophysical Obs.,* **15,** 11, 1955.

[14] J. G. Bolton and B. G. Clark, *Pub. A.S.P.,* **72,** 29, 1960.

TABLE I

960 Mc/s Source List A

Source		Right Ascension			Declination		
No.	Name	(1950)	Δ	Precession	(1950)	Δ	Precession
1	N.P.C.	$00^h02^m35^s$	$\pm30^s$	$+3^s\!.14$	+72°04′.5	± 4′	+0′.33
2	SN 1572	00 22 45.7	± 3	+3.34	+63 51.4	± 1	+0.33
3	3C 15	00 34 24	±10	+3.07	−01 20	± 4	+0.33
4	3C 17	00 35 40	± 8	+3.06	−02 23	± 4	+0.33
5	3C 20	00 39 56	±16	+3.37	+51 47	± 2	+0.33
6	NGC 281	00 50 05	±12	+3.43	+56 20.4	± 1.5	+0.33
7	3C 27	00 53 20	±15	+3.85	+68 00	± 3	+0.33
8	3C 28	(00 53 09.9	± 1)	+3.22	(+26 08.8	± 1)	+0.33
9	3C 32	01 05 47	±10	+2.96	−16 19.8	± 2*	+0.32
10	3C 33	01 06 21	± 5	+3.16	+13 06	± 3	+0.32
11	3C 38	01 18 05	±12	+2.95	−15 44	± 6	+0.32
12	3C 40	01 23 20	± 4	+3.06	−01 37.7	± 2	+0.31
13	3C 41	01 24 22	± 6	+3.38	+32 55	± 4	+0.31
14	3C 47	01 33 45	± 6	+3.22	+20 47	± 5	+0.31
15	3C 48	01 34 45	± 8	+3.42	+32 54.6	± 1.5	+0.31
16	3C 58	02 01 45	± 5	+4.50	+64 35.8	± 1.5	+0.29
17	3C 63	02 18 07	±10	+3.05	−02 12	± 6	+0.28
18	3C 66	02 19 49	± 4	+3.78	+42 45	± 3	+0.27
19	3C 75	02 54 55	± 6	+3.16	+05 53	± 3	+0.24
20	3C 79	03 07 07	± 8	+3.37	+16 54	± 2	+0.23
21	N.P.C.	03 16 22	±15	+3.28	+16 18.5	± 4	+0.23
22	NGC 1275	03 16 27	± 6*	+3.96	+41 21.3	± 1.5*	+0.22
23	Fornax A	03 20 25	±15	+2.30	−37 21.5	± 4	+0.22
24	3C 86	03 23 05	±15	+4.56	+55 06.8	± 2	+0.21
25	3C 89	03 31 26	±10	+3.05	−01 25	±10	+0.20
26	N.P.C.	03 36 54	±50*	+3.07	−01 55	± 8*	+0.19
27	3C 98	03 56 00	±10	+3.35	+10 19.7	± 2	+0.17
28	3C 103	04 04 39	±10	+4.18	+42 51.3	± 2.5	+0.16
29	3C 109	04 11 00	±15	+3.31	+11 07	± 4	+0.15
30	3C 111	04 15 06	± 8	+4.01	+37 53.3	± 1	+0.15
31	3C 123	04 33 50	± 3	+3.78	+29 34.1	± 1	+0.12
32	3C 129	04 45 40	±14*	+4.34	+44 56.4	± 4*	+0.11
33	HB 9	04 57 30	±30	+4.43	+46 26	± 4	+0.09
34	3C 134	05 01 12	±10*	+4.08	+38 00	± 4*	+0.09
35	Pictor A	05 18 19	±10	+1.72	−45 52	± 5	+0.06

TABLE I

960 Mc/s Source List A

No.	Intensity: Ratio to M 87	Intensity: [10^{-26} watts m^{-2} $(c/s)^{-1}$]	Relative Spectral Index	Optical Field
1	.043 ± .005	12.9 ± 1.5		
	(.25 ± .06)	(75 ± 18)		
2	.19 ± .01	57 ± 3	+0.19 ± 0.08	
3	.017 ± .004	5.1 ± 1.2	−0.06 ± 0.18	III
4	.034 ± .008	10.2 ± 2.4	+0.32 ± 0.26	IIa
5	.045 ± .005	13.5 ± 1.5	+0.13 ± 0.11	IV
6	.052 ± .004	15.6 ± 1.2		
	(.059 ± .006)	(17.7 ± 1.8)		
7	.036 ± .005	10.8 ± 1.5	+0.33 ± 0.17	IV
8	.008 ± .003	2.4 ± 0.9	−0.45 ± 0.22	IIb
9	.024 ± .005	7.2 ± 1.5	+0.16 ± 0.19	IIa
10	.060 ± .002	18 ± 0.6	+0.11 ± 0.07	I
11	.028 ± .005	8.4 ± 1.5	+0.19 ± 0.17	III
12	.027 ± .006	8.1 ± 1.8	+0.07 ± 0.20	I
13	.023 ± .003	6.9 ± 0.9	+0.59 ± 0.17	III
14	.021 ± .003	6.3 ± 0.9	−0.07 ± 0.16	IIa
15	.071 ± .006	21.3 ± 1.8	+0.28 ± 0.10	III
16	.111 ± .005	33.3 ± 1.5	+1.24 ± 0.15	IV
17	.020 ± .003	6.0 ± 0.9	+0.10 ± 0.13	III
18	.043 ± .003	12.9 ± 0.9	+0.30 ± 0.14	I
19	.025 ± .002	7.5 ± 0.6	+0.02 ± 0.10	I
20	.023 ± .002	6.9 ± 0.6	−0.09 ± 0.10	III
21	.030 ± .003	9.0 ± 0.9		III
22	.071 ± .007	21.3 ± 2.1	+0.06 ± 0.11	
23	.41 ± .02	123 ± 6		
	(.50 ± .04)	(150 ± 12)		
24	.040 ± .003	12 ± 0.9	+0.25 ± 0.10	IV
25	.021 ± .003	6.3 ± 0.9	+0.09 ± 0.18	IIa
26	.012 ± .004	3.6 ± 1.2		III
27	.047 ± .004	14.1 ± 1.2	+0.10 ± 0.10	I
28	.022 ± .002	6.6 ± 0.6	−0.18 ± 0.10	IV
29	.017 ± .003	5.1 ± 0.9	−0.03 ± 0.16	III
30	.068 ± .005	20.4 ± 1.5	+0.08 ± 0.09	IV
31	.215 ± .006	64.5 ± 1.8	+0.10 ± 0.07	IV
32	.031 ± .004	9.3 ± 1.2	−0.02 ± 0.12	III
33	.075 ± .015	22.5 ± 4.5		
	(.53 ± .10)	(160 ± 30)		
34	.050 ± .004	15.0 ± 1.2	−0.16 ± 0.10	IV
35	.280 ± .020	84 ± 6		

TABLE I (*Continued*)

Source		Right Ascension			Declination		
No.	Name	(1950)	Δ	Precession	(1950)	Δ	Precession
36	Crab Nebula	$05^h31^m30^s$		$+3^s.16$	$+21°59'.3$		$+0'.04$
37	Orion Nebula	05 32 49		+2.94	−05 25.3		+0.04
38	S 147	05 36		+3.78	+28		+0.03
39	3C 147	05 38 44	$\pm 6^s$	+4.65	+49 47	± 3′	+0.03
40	3C 154	06 10 23	±20*	+3.72	+26 03	± 7*	−0.01
41	IC 443	06 14 16	± 6*	+3.64	+22 36.4	± 3*	−0.02
42	3C 161	06 24 37	±10	+2.93	−05 51.4	± 2	−0.04
43	Rosette Nebula	06 29 24	±10	+3.19	+04 53	± 3	−0.04
44	3C 171	06 51 10	±15	+4.87	+54 12.4	± 2	−0.07
45	3C 196	08 10 02	±12	+4.34	+48 23	± 4	−0.18
46	Puppis A	08 21 20	±15	+2.06	−42 52	± 4	−0.19
47	Hydra A	09 15 43	± 2	+2.89	−11 52.4	± 1	−0.25
48	3C 227	09 44 59	± 8*	+3.17	+07 39	± 6*	−0.28
49	3C 234	09 58 26	±10*	+3.45	+29 02.4	± 4*	−0.29
50	3C 237	(10 05 21.9	± 1.5)	+3.16	(+07 43.8	± 2)	−0.29
51	3C 264	(11 42 34	± 6)	+3.11	(+20 00	± 9)	−0.33
52	3C 270	12 16 49	± 5	+3.06	+06 06	± 3	−0.33
53	3C 273	12 26 40	± 6	+3.07	+02 20	± 2	−0.33
54	M 87	12 28 18		+3.04	+12 40.1		−0.33
55	3C 278	(12 52 00	± 6)	+3.14	(−12 25	± 6)	−0.33
56	3C 279	(12 53 37	± 3)	+3.10	(−05 41	± 7)	−0.33
57	3C 280	(12 54 41.9	± 0.5)	+2.73	(+47 35.3	± 1)	−0.33
58	3C 283	13 08 50	±18*	+3.24	−22 11	± 5*	−0.32
59	NGC 5128	(13 22 28)		+3.51	(−42 45.6)		−0.31
60	3C 286	(13 28 49.7	± 1.5)	+2.77	(+30 45.6	± 1.5)	−0.31
61	3C 287	(13 29 04	± 3)	+2.82	(+25 24	± 6)	−0.31
62	3C 295	14 09 35	±12	+2.14	+52 25	± 3*	−0.28
63	3C 298	14 16 36	±12*	+2.98	+06 46	± 4*	−0.28
64	3C 310	15 02 30	±12*	+2.60	+26 12.5	± 2*	−0.23
65	3C 313	15 08 12	± 9*	+2.98	+08 03	± 4*	−0.23
66	3C 315	15 11 29	±10*	+2.58	+26 21	± 9*	−0.22
67	3C 317	15 14 14	±12	+2.95	+07 10	± 3	−0.22
68	3C 318	(15 17 52	± 6)	+2.69	(+20 28	± 5)	−0.22
69	3C 324	(15 47 34	± 5)	+2.63	(+21 33	± 7)	−0.18
70	3C 327	15 59 57	± 6*	+3.03	+02 04.6	± 3*	−0.17

TABLE I (*Continued*)

No.	Intensity: Ratio to M 87	Intensity: [10^{-26} watts m^{-2} $(c/s)^{-1}$]	Relative Spectral Index	Optical Field
36	3.43 ± .15	1030 ± 45	+0.51 ± 0.08	
37	1.20 ± .03	360 ± 9	+1.88 ± 0.06	
38	.043 ± .005	12.9 ± 1.5		
	(.4 ± .2)	(120 ± 60)		
39	.097 ± .003	29.1 ± 0.9	+0.25 ± 0.07	IV
40	.023 ± .002	6.9 ± 0.6	+0.18 ± 0.11	IV
41	.43 ± .02	129 ± 6	+0.54 ± 0.12	
	(.65 ± .08)	(195 ± 24)		
42	.080 ± .005	24.0 ± 1.5	+0.14 ± 0.09	IV
43	.350 ± .006	105 ± 2	+0.57 ± 0.20	
	(1.14 ± .12)	(342 ± 36)		
44	.020 ± .003	6.0 ± 0.9	+0.06 ± 0.18	III
45	.070 ± .005	21.0 ± 1.5	+0.02 ± 0.09	IIa
46	.34 ± .02	102 ± 6		
	(.44 ± .04)	(132 ± 12)		
47	.224 ± .006	67.2 ± 1.8	+0.09 ± 0.09	
48	.034 ± .003	10.2 ± 0.9	+0.07 ± 0.10	IIb
49	.024 ± .003	7.2 ± 0.9	−0.11 ± 0.12	IIb
50	.018 ± .003	5.4 ± 0.9	−0.09 ± 0.14	III
51	.035 ± .010	10.5 ± 3.0	+0.18 ± 0.20	IIa
52	.095 ± .005	28.5 ± 1.5	+0.93 ± 0.19	I
53	.167 ± .008	50.1 ± 2.4	+0.47 ± 0.15	III
54		300	0.00 ± 0.08	
55	.032 ± .005	9.6 ± 1.5	−0.10 ± 0.19	I
56	.023 ± .004	6.9 ± 1.2	+0.11 ± 0.18	III
57	.023 ± .004	6.9 ± 1.2	−0.02 ± 0.15	III
58	.034 ± .005	10.2 ± 1.5	+0.02 ± 0.19	III
59	1.54 ± .10	462 ± 30		
	(6.7 ± .5	(2010 ±150)		
60	.065 ± .005	19.5 ± 1.5	+0.62 ± 0.09	III
61	.028 ± .004	8.4 ± 1.2	+0.04 ± 0.18	III
62	.102 ± .008	30.6 ± 2.4	+0.19 ± 0.10	III
63	.037 ± .005	11.1 ± 1.5	−0.08 ± 0.13	III
64	.036 ± .006	10.8 ± 1.8	−0.28 ± 0.14	I
65	.018 ± .003	5.4 ± 0.9	−0.32 ± 0.14	III
66	.020 ± .003	6.0 ± 0.9	−0.10 ± 0.21	I
67	.033 ± .003	9.9 ± 0.9	−0.16 ± 0.10	IIa
68	.009 ± .003	2.7 ± 0.9	−0.20 ± 0.24	III
69	.021 ± .005	6.3 ± 1.5	+0.12 ± 0.24	III
70	.039 ± .007	11.7 ± 2.1	−0.03 ± 0.14	IIa

TABLE I (*Concluded*)

Source		Right Ascension			Declination		
No.	Name	(1950)	Δ	Precession	(1950)	Δ	Precession
71	3C 330	$16^h09^m05^s$	$\pm 20^s$	$+0^s.40$	+66°05′	± 3′	$-0'.16$
72	3C 338	16 26 54	±10	+2.06	+39 35.3	± 2.5	−0.13
73	3C 343	16 36 56	±14*	+0.65	+62 41.7	± 2.5	−0.12
74	3C 345	16 41 57	± 5	+2.02	+39 53.5	± 2	−0.11
75	Hercules A	16 48 43	± 2	+2.96	+05 06.4	± 0.5	−0.10
76	3C 353	17 17 59	± 3	+3.05	−00 55.5	± 1.5	−0.06
77	MSH 17−1<u>6</u>	(17 19 24	±30)	+3.52	(−18 45	± 7)	−0.06
78	SN 1604	(17 27 47	± 5)	+3.58	(−21 16	±10)	−0.05
79	3C 380	18 28 17	± 8	+1.56	+48 41	± 2	+0.04
80	N.P.C.	18 33 21	± 6	+2.22	+32 40.6	± 1	+0.05
81	3C 386	18 36 13	± 8	+2.75	+17 05.5	± 2	+0.05
82	3C 388	18 42 31	± 9	+1.74	+45 28	± 3	+0.06
83	3C 392	(18 53 35	± 5)	+3.05	(+01 15	± 7)	+0.07
84	3C 398	(19 08 44.4	± 1.5)	+2.87	(+09 05	± 4)	+0.10
85	3C 401	19 40 21	±20	+0.92	+60 33.4	± 3	+0.14
86	3C 402	(19 40 23	± 7)	+1.60	(+50 32	± 8)	+0.14
87	3C 403	19 49 38	±16	+3.03	+02 21.7	± 2	+0.15
88	Cygnus A	19 57 44.5		+2.08	+40 35.8		+0.16
89	3C 409	20 12 18	±10*	+2.59	+23 25	± 3*	+0.18
90	3C 410	20 18 01	±15	+2.45	+29 33.5	± 1	+0.19
91	HB 21	20 45		+1.85	+50 30		+0.22
92	3C 424	(20 45 43	± 4)	+2.95	(+06 50	± 6)	+0.22
93	Cygnus Loop	20 50		+2.50	+30		+0.23
94	3C 430	21 16 34	± 8	+1.52	+60 36	± 1.5	+0.25
95	3C 433	21 21 30	±10	+2.68	+24 50.3	± 3	+0.26
96	3C 436	21 42 01	±10	+2.67	+27 54	± 6	+0.28
97	N.P.C.	21 51 37	± 7*	+2.30	+46 50	± 3*	+0.28
98	3C 438	21 53 54	± 6	+2.53	+37 43.4	± 2	+0.28
	3C 442	(22 10 30	± 4)	+2.95	(+10 50	± 6)	+0.30
99	3C 444	22 11 33	± 8	+3.26	−17 13.7	± 3	+0.29
100	3C 445	22 21 17	±12	+3.10	−02 27	± 4	+0.30
101	3C 446	22 23 03	±10	+3.13	−05 14.6	± 3	+0.30
102	N.P.C.	22 29 53	± 6	+2.97	+11 28.2	± 2	+0.31
103	3C 452	22 43 33	±10	+2.71	+39 25	± 3	+0.32
104	3C 459	23 13 57	± 6	+3.05	+03 49	± 3	+0.33
105	Cassiopeia A	23 21 11.4		+2.71	+58 31.9		+0.33
106	3C 465	23 35 53	± 8	+3.00	+26 46.3	± 3	+0.33

TABLE I (*Concluded*)

No.	Intensity: Ratio to M 87	Intensity: [10^{-26} watts m^{-2} $(c/s)^{-1}$]	Relative Spectral Index	Optical Field
71	.029 ± .005	8.7 ± 1.5	+0.15 ± 0.15	III
72	.024 ± .004	7.2 ± 1.2	−0.37 ± 0.14	I
73	.035 ± .003	10.5 ± 0.9	+0.43 ± 0.12	III
74	.028 ± .004	8.4 ± 1.2	+0.70 ± 0.15	IIa
75	.245 ± .020	73.5 ± 6	−0.19 ± 0.10	
76	.279 ± .006	83.7 ± 1.8	+0.17 ± 0.06	III
77	.017 ± .006	5.1 ± 1.8		IV
	(.12 ± .08)	(36 ± 24)		
78	.065 ± .007	19.5 ± 2.1	+0.12 ± 0.15	
79	.061 ± .002	18.3 ± 0.6	+0.03 ± 0.07	III
80	.023 ± .002	6.9 ± 0.6		IIa
81	.032 ± .002	9.6 ± 0.6	+0.17 ± 0.09	III
82	.033 ± .004	9.9 ± 1.2	+0.28 ± 0.13	III
83	.703 ± .030	211 ± 9	+0.29 ± 0.08	IV
84	.30 ± .06	90 ± 18	+0.85 ± 0.16	IV
85	.026 ± .003	7.8 ± 0.9	+0.15 ± 0.13	III
86	.015 ± .004	4.5 ± 1.2	+0.04 ± 0.22	IIa
87	.032 ± .002	9.6 ± 0.6	+0.23 ± 0.15	IV
88	7.2 ± .4	2160 ±120	−0.09 ± 0.08	
89	.073 ± .004	21.9 ± 1.2	−0.03 ± 0.08	IV
90	.043 ± .003	12.9 ± 0.9	+0.07 ± 0.13	IV
91	.20 ± .02	60 ± 6		
	(.6 ± .2)	(180 ± 60)		
92	.021 ± .003	6.3 ± 0.9	+0.22 ± 0.19	III
93	.11 ± .01	33 ± 3		
	(.84 ± .15)	(252 ± 45)		
94	.037 ± .005	11.1 ± 1.5	−0.50 ± 0.24	III
95	.051 ± .005	15.3 ± 1.5	−0.07 ± 0.11	I
96	.021 ± .002	6.3 ± 0.6	+0.06 ± 0.13	IV
97	.015 ± .002	4.5 ± 0.6		IV
98	.035 ± .002	10.5 ± 0.6	−0.16 ± 0.09	IV
	not detected			
99	.045 ± .002	13.5 ± 0.6	+0.02 ± 0.12	IIa
100	.027 ± .004	8.1 ± 1.2	+0.15 ± 0.13	IIa
101	.026 ± .003	7.8 ± 0.9	+0.29 ± 0.12	III
102	.024 ± .002	7.2 ± 0.6		IIa
103	.046 ± .003	13.8 ± 0.9	−0.09 ± 0.09	III
104	.024 ± .002	7.2 ± 0.6	+0.02 ± 0.14	III
105	10.4 ± .5	3120 ±150	−0.05 ± 0.08	
106	.039 ± .003	11.7 ± 0.9	+0.08 ± 0.10	IIa

Notes to Table I

The first column lists a serial number and the second column gives the source name. The sources are usually designated by the 3C number, except where a more common term such as the optical name is well known. Sources not previously catalogued are indicated by "N.P.C.," except for unquestionable identifications such as NGC 281. It is suggested that N.P.C. sources be referred to as "CTA" followed by the serial number. "CT" is an abbreviation for "Caltech" and the letter "A" denotes the first list of radio sources published by this observatory.

The next six columns give the position of the source together with the estimated errors (Δ) and the annual precession. An asterisk indicates that the value is the result of a single observation. Positions in parentheses are those given by the previous observer and indicate that no measurement of position was made in the present study.

The intensity is tabulated both as a ratio to M 87 and as a flux density based on a value of 300×10^{-26} watts $m^{-2}(c/s)^{-1}$ for M 87. For sources of appreciable size the peak intensity is given first, followed by the integrated intensity in parentheses.

Next is given the relative spectral index, $(x - x_{M87})$, computed from the Cambridge and Caltech intensities. The final column lists the optical field class defined in Section V.

Remarks on individual sources follow. Sources that appear in other catalogues are indicated by MSH (Mills, Slee, and Hill[8]), W (Westerhout[11]) or HB (Hanbury Brown and Hazard[12]).

CTA 1: Faint wisp of emission on Schmidt plate agrees with radio-intensity distribution. Possibly supernova remnant.
NGC 281: H II region.
3C 32: MSH $01-1\underline{2}$.
3C 33: Isolated elliptical galaxy.
3C 38: MSH $01-1\underline{9}$.
3C 40: MSH $01-0\underline{5}$. Pair of bright elliptical galaxies NGC 545/547.
3C 58: Spectral index, source size (preliminary Caltech interferometer result), and galactic latitude (+4°) indicate a galactic source.
3C 63: MSH $02-0\underline{7}$.
3C 66: Elliptical galaxy that may have a jet (Minkowski, private communication).
3C 75: MSH $02+01\underline{0}$. Pair of elliptical galaxies.
CTA 21: Rising background to north.
3C 89: MSH $03-0\underline{3}$.
3C 98: Elliptical galaxy.
3C 123: W 7, IAU 04N3A.
Crab Nebula: Optical position given (calibrator).

Orion Nebula: Optical position given (calibrator).
S 147: Possible supernova remnant; source No. 74 of Gaze and Shaĭn.[13]
3C 161: MSH 06 − 04.
Rosette Nebula: Weak extensions to the north and east agreeing with optical emission.
3C 227: MSH 09 + 07.
3C 237: MSH 10 + 01.
3C 264: Preliminary interferometer observations indicate one source near the 3C position rather than the two sources that Elsmore observed.
3C 270: MSH 12 + 05. Elliptical galaxy NGC 4261.
3C 273: MSH 12 + 08, W 17.
M 87: Optical position given (calibrator).
3C 278: MSH 12 − 118. Pair of elliptical galaxies NGC 4782/4783.
3C 279: MSH 12 − 020.
NGC 5128: Centaurus A. Optical position given. Intensity based in part on Bolton and Clark.[14]
3C 298: MSH 14 + 05.
3C 310: Pair of elliptical galaxies.
3C 313: MSH 15 + 02.
3C 317: MSH 15 + 05.
3C 324: Confused by an extended source approximately 7^m later in right ascension.
3C 327: MSH 16 + 01.
3C 338: Multiple system of elliptical galaxies, NGC 6166.
3C 353: MSH 17 − 06, W 21.
MSH 17 − 16: May be two sources.
CTA 80: Source on intervening declination lobe between 3C 382 and 3C 384.
3C 392: MSH 18 + 011, W 44.
3C 398: W 49. Spectral index, source size (4′ Elsmore *et al.*[7]), and galactic latitude (−2°) indicate a galactic source.
3C 403: MSH 19 + 010.
Cygnus A: Optical position given (calibrator).
3C 424: MSH 20 + 010.
3C 433: Pair of galaxies.
CTA 97: Radio position just south of IC 5146, an H II region with a diffuse blue extension.
3C 444: MSH 22 − 17.
3C 445: MSH 22 − 09.
3C 459: MSH 23 + 05.
Cassiopeia A: Optical position given (calibrator).